



# High-Temperature Measurements on Viscosity and Surface Tension of the Ionic Liquid 1-Ethyl-3-methylimidazolium Bis(trifluoromethylsulfonyl)imide ([EMIM][NTf<sub>2</sub>]) up to 473 K

Ziwen Zhai<sup>1</sup> · Thomas M. Koller<sup>1</sup>

Received: 2 June 2023 / Accepted: 6 June 2023 / Published online: 30 June 2023  
© The Author(s) 2023

## Abstract

In the present study, the viscosity and surface tension of the commercial low-viscosity ionic liquid (IL) 1-ethyl-3-methylimidazolium bis(trifluoromethylsulfonyl)imide ([EMIM][NTf<sub>2</sub>]) were determined by a combination of surface light scattering (SLS) and the pendant-drop (PD) method between (303 and 473) K. Both methods operating at thermodynamic equilibrium were applied inside the same measurement cell at identical experimental conditions under an argon atmosphere at 0.1 MPa. For SLS measurements performed in the temperature range from (303 to 323) K, the overdamped behavior of the surface fluctuations allowed access to the viscosity with an expanded uncertainty of 2.3 % using the surface tensions determined via the PD method with an uncertainty of 2 % as input quantities. Above 323 K up to 473 K, the oscillatory behavior of the probed surface fluctuations by SLS enabled a simultaneous determination of viscosity and surface tension with average expanded uncertainties of (4 and 3) %, respectively. Multiple repetition measurements by both methods have been conducted at 323 K after experiments at larger temperatures up to 473 K, and the consistency of their results could indicate a sound thermal stability of the IL sample. The mutual agreement of the surface tension results from SLS and the PD method between (353 and 473) K demonstrates that both techniques analyze the very same IL surface. For both properties, the results from this work agree well with the majority of experimental data reported in the literature typically up to 353 K. In summary, the viscosity and surface tension results presented in this study contribute to an improved data landscape for this particular IL and ILs in general at elevated temperatures.

**Keywords** [EMIM][NTf<sub>2</sub>] · Ionic liquid · Pendant-drop method · Surface light scattering · Surface tension · Viscosity

## 1 Introduction

Ionic liquids (ILs) are electrolytes that feature a liquid state typically below 100 °C and often even at room temperature. Due to the wide number of potential combinations of cations and anions as well as their interesting properties such as the extremely low vapor pressure, ILs are interesting working fluids for various applications in research and industry [1–4]. In the field of reaction engineering, for example, ILs may serve as liquid containers for performing many industrially important catalytic processes including hydrogenation, dehydrogenation, or hydroformylation [3–6]. Since these reactions appear often at relatively large temperatures around 393 K or above, the characterization of the involved ILs *via* their thermophysical properties at process-relevant conditions is of significant relevance for the design and optimization of processes and process equipment. The present study focuses on viscosity as the transport property for the description of momentum transfer and on surface tension as the key equilibrium property for the characterization of fluid interfaces.

As a representative model system, the commercially available IL 1-ethyl-3-methylimidazolium bis(trifluoromethylsulfonyl)imide (often abbreviated by [EMIM][NTf<sub>2</sub>] in literature) has been chosen here due to its interesting properties for aforementioned applications such as a wide electrochemical window [7], a relatively low viscosity, its hydrophobicity, and a high degree of thermal stability. According to the literature [8], [EMIM][NTf<sub>2</sub>] has been categorized as “most stable” with respect to long-term thermal stability, i.e., only 1 % mass loss was observed over a 10 h duration at an elevated temperature of 495 K. For this IL, an extensive research on the thermophysical properties has already been conducted, also with respect to viscosity and surface tension, which is documented in the “NIST Ionic Liquids Database—ILThermo” [9]. As will be addressed in the present work, the partly observed discrepancies among published experimental data sets for ILs seem to originate from differences in the sample characteristics and/or the improper application of experimental techniques. Furthermore, the literature survey reveals that only a limited number of viscosity [10–14] and surface tension [12, 15, 16] data is available for [EMIM][NTf<sub>2</sub>] at temperatures above 353 K. This lack of information is the common situation for ILs [9] and complicates the understanding of their fluid behavior at elevated temperatures.

In former studies, e.g., in Refs. [17–19], it could be shown that surface light scattering (SLS) allows for a reliable determination of the viscosity of ILs with an expanded (coverage factor  $k=2$ ) uncertainty of 3 % and below. In comparison to conventional techniques, the main advantage of the SLS technique is the possibility of determining the viscosity and, for fluids of relatively low viscosity, also the surface or interfacial tension in macroscopic thermodynamic equilibrium in an absolute way without any calibration procedure [20, 21]. Recently [22], the SLS technique could be combined with conventional tensiometry in the form of the pendant-drop (PD) method within one setup, which offers the opportunity to investigate the very same samples by both measurement principles. This is particularly beneficial for ILs with their commonly large viscosities, where the

evaluation of the SLS signals requires information on the surface tension to determine the viscosity. Under such conditions, the determination of viscosity and surface tension by the combination of SLS and the PD method could be realized for ILs and IL mixtures at gas pressures between (0.02 and 10) MPa and temperatures between (303 and 393) K [22–24].

The main objective of the present study is to extend the investigations on ILs by conducting combined SLS and PD experiments at temperatures up to 473 K, which provides multiple advantages. First, it allows for the evaluation of the thermal stability of a dried [EMIM][NTf<sub>2</sub>] sample under a controlled inert gas atmosphere of argon at 0.1 MPa. Once the thermal stability is confirmed, the application of elevated temperatures can be utilized to study a range of sufficiently low IL viscosities, where SLS experiments allow for a simultaneous determination of viscosity and surface tension. The latter property can then be compared directly with corresponding results obtained from the PD method. Furthermore, corresponding experiments can provide an extension of the available database for viscosity and surface tension of the IL [EMIM][NTf<sub>2</sub>] with respect to higher temperatures.

## 2 Theoretical Background

In this section, the principles of the SLS technique and PD method are briefly summarized. A detailed description on the hydrodynamic theory behind SLS and its experimental realization for the determination of viscosity and/or surface or interfacial tension of two-phase systems can be found in literature, see, e.g., in Refs. [20, 21, 25]. In connection with the PD method, a fundamental discussion on the theory and proper execution of this type of tensiometer is provided in Ref. [26].

In SLS, the dynamics of surface fluctuations, also called capillary waves, present at the phase boundary between two fluid phases can be analyzed at macroscopic thermodynamic equilibrium. These dynamics are accessible by analyzing the light scattered from the phase boundary at a specified modulus of the wave vector  $q$ . Using photon correlation spectroscopy, the measured time-dependent correlation functions (CF) of the scattered light intensity reflects the temporal behavior of the surface fluctuations, which is characterized by their decay time  $\tau_C$  and their propagation frequency  $\omega_q$ . This observed temporal behavior gives rise to two different scenarios, namely, the overdamped behavior ( $\omega_q=0$ ) or the oscillatory behavior ( $\omega_q\neq 0$ ), which can be differentiated by the dimensionless capillary number  $Y$ . This quantity depends on the probed  $q$  and several thermophysical properties of fluid including the liquid dynamic viscosity  $\eta_L$  and the surface tension  $\sigma$ . For  $Y < 0.145$ , corresponding to large  $\eta_L$  and small  $\sigma$ , the surface fluctuations show an overdamped behavior, and the predominantly present mode with the characteristic decay time  $\tau_C$  gives typically only access to the ratio of  $\eta_L$  to  $\sigma$ . For  $Y > 0.145$ , i.e., small  $\eta_L$  and large  $\sigma$ , the surface fluctuations are characterized by an oscillatory behavior reflected by both  $\tau_C$  and  $\omega_q$ . For the accurate determination of  $\eta_L$  and  $\sigma$ , the dispersion relation for surface fluctuations at the gas–liquid phase boundary [21, 27] needs to be used in its complete form, as it has been carried out in the present work. For this,

also reference data for the liquid density  $\rho_L$ , the gas density  $\rho_G$ , and the gas viscosity  $\eta_G$  were considered.

In addition to SLS, the PD method has been used for the determination of  $\sigma$ . At thermodynamic equilibrium, the shape of a liquid droplet exposed to a surrounding gas atmosphere and hanging on the tip of, for example, a capillary is governed by the competition between the gravitational force due to the gravitational field and the capillary force caused by  $\sigma$ . Based on axisymmetric drop shape analysis (ADSA) [28], the evaluation of  $\sigma$  is performed by comparing the experimentally recorded droplet contour with the theoretically defined droplet geometry described by the Young–Laplace (YL) equation [26]. Details to this evaluation procedure can be found in Ref. [29]. Besides the geometric calibration of the optical system, which allows for the pixel-to-metric scale conversion, the information about  $\rho_L$  and  $\rho_G$  are required to solve the YL equation. The data for  $\sigma$  obtained by the PD method were also used to evaluate  $\eta_L$  from SLS experiments in the overdamped case.

### 3 Experimental Section

#### 3.1 Sample Preparation and Measurement Procedure

A sample of the IL 1-ethyl-3-methylimidazolium bis(trifluoromethylsulfonyl)imide ([EMIM][NTf<sub>2</sub>], molar mass  $M=391.31\text{ g}\cdot\text{mol}^{-1}$ ) was purchased from IoLiTec (Ionic Liquids Technologies GmbH) with a purity of 99.5 % and a specified water content of less than 100 ppm. By subjecting the sample to a degassing process at about 0.5 Pa and 323 K for 4 h, the water content could be further reduced to 47 ppm, as analyzed by a Karl-Fischer coulometer. Subsequently, the degassed sample was transferred to the experimental setup, and the experiments were conducted under an argon (Ar) atmosphere. This gas was delivered by Linde AG with a volume fraction purity of more than 0.99999.

Combined SLS and PD measurements were performed within a setup specifically designed for this task. A detailed description of the SLS-PD setup can be found in our previous study [22]. Prior to the measurements, the sample cell made of stainless steel was filled with the pure and dried IL sample, and flushed with Ar by adjusting a pressure of around 0.1 MPa measured by a pressure transducer. By applying resistance heating and several Pt-100 temperature probes, the temperature of the sample cell could be adjusted to a stability below  $\pm 6\text{ mK}$  up to 373 K, which increased up to  $\pm 80\text{ mK}$  at 473 K. The reported temperature  $T$  refers to the temperature measured in the gas phase next to the PDs produced in the upper part of the cell *via* a connected syringe. In the bottom part of the cell, a liquid sample of about 20 mL is used for SLS measurements. The uncertainty in  $T$  can be interpolated linearly between (0.02 to 0.50) K in the investigated temperature range from (303 to 473) K. This conservatively stated uncertainty considers the uncertainty of the probe itself, the  $T$  stability, and the deviations in temperature between the probe in the gas phase used for the specification of  $T$  and in the stainless steel cell underneath the liquid phase, as detailed in Ref. [22]. Once equilibrium conditions were reached, PD and SLS measurements were performed in a consecutive manner at eleven temperatures

in the range from (303 to 473) K by a stepwise increase of  $T$ . In the case of the PD measurements, the reported  $\sigma$  results represent the mean averages of 25 individual images captured from 5 drops for each thermodynamic state. The maximum deviation of the 25 individual values for  $\sigma$  was found to be always less than 1 %. For the heterodyne SLS experiments performed in reflection direction, where the scattered light is detected perpendicularly to the gas–liquid interface, four single measurements associated with different moduli for  $q$  between  $(5.11$  and  $6.59) \times 10^5 \text{ m}^{-1}$  were conducted for each  $T$ . By forming the mean averages of the corresponding results, the final values for  $\eta_L$  in the overdamped case and for  $\eta_L$  and  $\sigma$  in the oscillatory case were obtained.

To control the thermal stability of the sample, regular repetition measurements were conducted at 323 K after experiments at larger  $T$ . After these repetitions, the temperature was again increased to the next larger value. A detailed discussion on this issue is given in Sect. 4.1. For performing the combined SLS-PD experiments at each temperature state, the measurement time was on the order of 4 h. The entire measurement period including several temperature loops lasted about one and a half week.

### 3.2 SLS Measurement Examples

To visualize the two different temporal behaviors of the surface fluctuations at the interface between the IL [EMIM][NTf<sub>2</sub>] and Ar, Fig. 1 shows two CFs recorded by SLS experiments at the lowest (left part) and highest (right part)

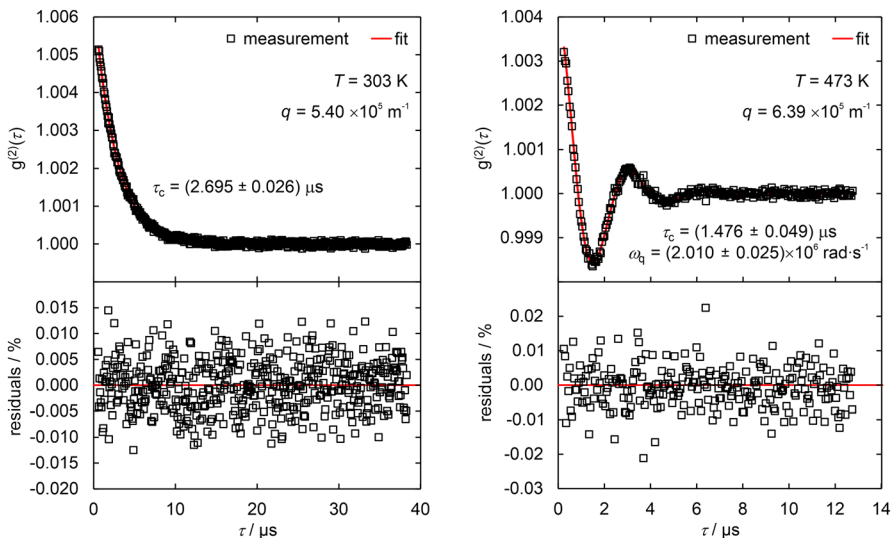


**Fig. 1** Measurement examples of the normalized CFs (upper part) and their residuals (lower part) for [EMIM][NTf<sub>2</sub>] as a function of delay time  $\tau$  obtained from SLS experiments in reflection direction with an overdamped behavior at  $T=303$  K (left) and an oscillatory behavior at  $T=473$  K (right)

temperatures investigated in this study. At 303 K, the CF on the left side obtained at  $q = 5.40 \times 10^5 \text{ m}^{-1}$  reflects an overdamped behavior ( $Y \approx 0.034$ ). Based on a single exponentially decaying function applied to the measured CF, a decay time and related expanded ( $k=2$ ) uncertainty  $\tau_C = (2.695 \pm 0.026) \mu\text{s}$  are obtained by fit. Such an overdamped behavior was observed for temperatures between (303 and 323) K. At 333 K, the transition from the overdamped to the oscillatory case in the region near the critical damping ( $Y \approx 0.145$ ) took place, where the representation of the CF is very challenging and only possible with relatively large uncertainties. As a result, no SLS results are reported here. Starting from 353 K, a clear oscillatory behavior of surface fluctuations was found, as it can also be seen in the right part of Fig. 1 for 473 K. To represent this CF ( $Y \approx 4.8$ ) and all other CFs in the oscillatory case, the influence of the rotational flow in the liquid bulk of the fluid on the damped oscillation signal had to be considered in accordance with the evaluation strategy discussed in Ref. [30]. As a result, accurate  $\tau_C$  and  $\omega_q$  data with typical relative uncertainties of 3 % and 1 %, respectively, could be extracted from the experimental SLS signals. In both scenarios, the residual plots showing the deviations of the measured from the fitted data in the lower part of Fig. 1 are free of any systematics, which indicates the validity of the theoretical working equations.

## 4 Results and Discussion

The results of the liquid dynamic viscosity  $\eta_L$  and surface tension  $\sigma$  of [EMIM][NTf<sub>2</sub>] for temperatures  $T$  between (303 and 473) K obtained from combined SLS-PD experiments are summarized in Table 1. Therein, also the input parameters for liquid density  $\rho_L$ , vapor density  $\rho_G$ , and vapor viscosity  $\eta_G$  are included. Here,  $\rho_L$  was obtained using the fit equation determined from density measurements by Tariq *et al.* [15] at 0.1 MPa in the temperature range from (293 to 473) K, which are accompanied by a reported uncertainty of 0.4 %. The influence of the Ar gas pressure of 0.1 MPa on  $\rho_L$  can safely be neglected. Considering the extremely low vapor pressure of ILs, the gas phase is given by pure Ar, for which the gas properties  $\rho_G$  and  $\eta_G$  were calculated using the REFPROP database [31] at the specified measurement conditions in terms of temperature and pressure. The corresponding expanded ( $k=2$ ) uncertainties for  $\rho_G$  and  $\eta_G$  can be found in the caption of Table 1. In line with our previous studies [22, 23, 32], the expanded ( $k=2$ ) uncertainty for the reported surface tension data from PD method is specified to be 2.0 %. This uncertainty sufficiently accounts for the uncertainty related to the used correlation for  $\rho_L$  and is also considered in the evaluation of  $\eta_L$  and its uncertainty from SLS measurements in the overdamped case. The corresponding uncertainties for the SLS results were calculated from error propagation schemes considering the uncertainties of the relevant input parameters. More details to these schemes are reported in Ref. [22]. By averaging over the individual uncertainties within the overdamped and oscillatory region, expanded ( $k=2$ ) uncertainties of 2.3 % for  $\eta_L$  in the overdamped case as well as of 4.0 % and 3.0 % for  $\eta_L$  and  $\sigma$ , respectively, in the oscillatory case were obtained.

**Table 1** Liquid viscosity  $\eta_L$  and surface tension  $\sigma$  of [EMIM][NTf<sub>2</sub>] in the presence of an Ar atmosphere at around 0.1 MPa as a function of temperature  $T$  obtained by PD method and SLS using input data for the liquid density  $\rho_L$ , gas density  $\rho_G$ , and gas viscosity  $\eta_G$

$T$ (K)	$\rho_L$ (kg·m <sup>-3</sup> )	$\rho_G$ (kg·m <sup>-3</sup> )	$\rho_G$ (μPa·s)	$\sigma_{PD}$ (mN·m <sup>-1</sup> )	$100 \cdot U_r(\sigma_{PD})$	$\sigma_{SLS}$ (mN·m <sup>-1</sup> )	$100 \cdot U_r(\sigma_{SLS})$	$\eta_L$ (mPa·s)	$100 \cdot U_r(\eta_L)$
303.12	1517.08	1.74	22.9	36.06	2.0	—	—	27.54	2.3
312.98	1506.77	1.69	23.6	35.48	2.0	—	—	20.13	2.3
323.13	1493.45	1.64	24.2	35.00	2.0	—	—	15.57	2.3
333.18	1483.52	1.69	24.8	34.50	2.0	—	—	—	—
353.21	1465.43	1.73	24.8	33.52	2.0	33.04	3.0	7.80	4.0
373.13	1445.38	1.63	26.0	32.59	2.0	33.01	3.0	5.65	4.0
392.99	1425.67	1.67	27.2	31.57	2.0	31.78	3.0	4.25	4.0
413.09	1405.99	1.59	28.3	30.69	2.0	31.36	3.0	3.32	4.0
433.04	1386.73	1.63	29.4	29.74	2.0	30.39	3.0	2.66	4.0
453.23	1367.50	1.55	30.5	28.83	2.0	28.94	3.0	2.09	4.0
473.38	1348.58	1.59	31.6	27.90	2.0	28.00	3.0	1.80	4.0

The uncertainties for  $T$  can be linearly interpolated between  $U_r(T) = (0.02 \text{ and } 0.50) \text{ K}$  in the investigated  $T$  range from (303 to 473) K. Data for  $\rho_L$  are calculated based on experiment-based fit correlation in Ref. [15] with a relative expanded ( $k=2$ ) uncertainty  $U_r(\rho_L) = 0.4\%$ . The employed properties for  $\rho_G$ , and  $\eta_G$  of Ar with relative expanded ( $k=2$ ) uncertainties  $U_r(\rho_G) = 0.2\%$  and  $U_r(\eta_G) = 0.5\%$  are obtained from the Ref. [31] at the specific temperature and pressure during the measurement. For the liquid dynamic viscosity and surface tension, the relative expanded ( $k=2$ ) uncertainties  $U_r(\eta_L)$  and  $U_r(\sigma_{SLS})$  obtained from SLS measurements and  $U_r(\sigma_{PD})$  obtained from PD method are given in the table

In the following, the thermal stability of the IL sample up to 473 K is first validated by analyzing the thermophysical property results from several repetition measurements. Thereafter, the results for viscosity and surface tension of [EMIM][NTf<sub>2</sub>] listed in Table 1 are represented by temperature-dependent correlations and are discussed. Here, a particular focus is on the comparison of the experimental data available in literature for viscosity and surface tension at or close to ambient pressure of 0.1 MPa with the present results.

#### 4.1 Check of Thermal Stability

To probe the thermal stability of the studied [EMIM][NTf<sub>2</sub>] sample up to elevated temperatures of 473 K, a couple of repetition measurements by SLS and the PD method were conducted at 323 K. The measurements were performed after corresponding measurements at larger temperatures of (373, 413, 453, and 473) K, i.e., four temperature cycles were carried out. In Fig. 2, the relative deviations of the results for the surface tension  $\sigma$  (left part) and liquid viscosity  $\eta_L$  (right part) determined from the repetition PD and SLS measurements at 323 K, relative to the corresponding reference values obtained from the initial measurements at 323 K, are shown in the form of bar diagrams. These reference values refer to the fit values  $\eta_{L,calc}$  and  $\sigma_{calc}$  developed from the  $T$ -dependent measurement results in Sects. 4.2 and 4.3, respectively. As can be seen in Fig. 2, the repetition results are always within  $\pm 1.0\%$  for surface tension and within  $\pm 1.2\%$  for viscosity in comparison to the initial values. These deviations are smaller than the related expanded uncertainties of the individual data indicated by the dashed lines in both parts of Fig. 2 for the reference values. All these findings indicate a certified long-time thermal stability of [EMIM][NTf<sub>2</sub>] up to 473 K under an inert gas atmosphere over the total measurement period. Such statement is in agreement with studies [8, 33, 34] on the thermal stability of this particular IL, and ensures the reliability of the present viscosity and surface tension results.

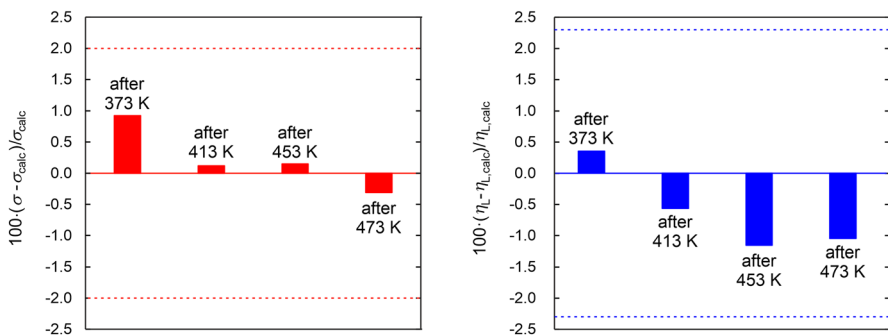


**Fig. 2** Bar diagrams showing the relative percentage deviation of the results from the repetition measurements for the surface tension (left, measured by PD method) and viscosity (right, measured by SLS) at 323 K after investigations at elevated temperatures of (373, 413, 453, and 473) K, relative to the initial values  $\sigma_{calc}$  and  $\eta_{L,calc}$  obtained at 323 K. In both plots, the dashed lines represent the expanded ( $k=2$ ) uncertainties for the reference values of the corresponding property



## 4.2 Liquid Viscosity

The SLS results for the liquid dynamic viscosity  $\eta_L$  of [EMIM][NTf<sub>2</sub>] listed in Table 1 are plotted as a function of  $T$  in the upper part of Fig. 3. They cover a broad viscosity range from (28 down to 2) mPa·s, show the typical decreasing behavior with increasing temperature, and could be correlated well by a Vogel-type equation according to

$$\eta_{L,\text{calc}}(T) = \eta_0 \exp(B/(T - C)). \quad (1)$$

By unweighted fitting of all the experimental data in the entire  $T$  range *via* a least-squares minimization algorithm, the three fit parameters of Eq. 1 are determined to be  $\eta_0 = 0.11220$  mPa·s,  $B = 957.13$  K, and  $C = 128.89$  K. The average absolute relative deviation (AARD) of the measured data from Eq. 1 is 1.3 %. As

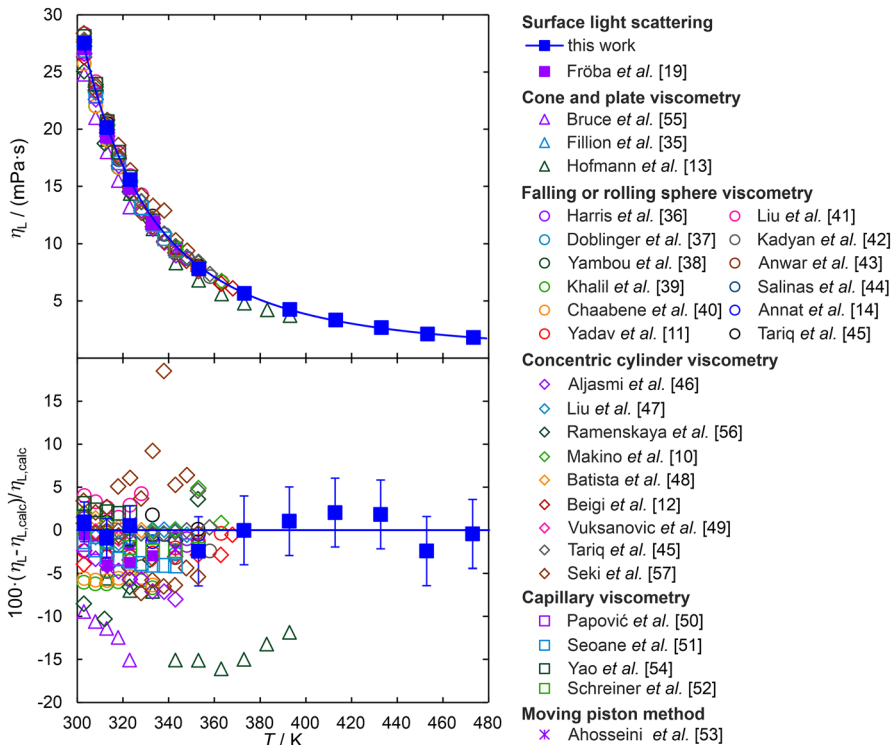


**Fig. 3** Data comparison for liquid dynamic viscosity  $\eta_L$  of [EMIM][NTf<sub>2</sub>] at 0.1 MPa as a function of temperature  $T$ . The upper part presents the absolute values obtained from the present SLS measurements (■) as well as collected from literature and categorized according to the used measurement technique, while the lower part shows the relative deviations of the experimental data from the fit  $\eta_{L,\text{calc}}$  (—, Eq. 1) developed from the present SLS results. Error bars representing the experimental expanded ( $k=2$ ) uncertainties are only shown for the present SLS data (Color figure online)

can be seen from the lower part of Fig. 3, the relative deviations of the SLS data from  $\eta_{L,calc}$  are always smaller than their uncertainties indicated by the error bars.

In Fig. 3, the viscosity values obtained in this study are also compared with the experimental data in literature from in total 30 different Refs. [10–14, 19, 35–58], which were collected from the IL database “ILThermo” [9] since the year 2008 and include at least 3 data points per set. These database encompasses various types of used viscometers, as classified by different marker types in Fig. 3. According to the lower part of Fig. 3, our viscosity data are generally in the middle of the literature values determined in most cases only up to about 353 K. Particularly, good agreement within about  $\pm 5\%$  is observed with the results from former SLS experiments limited to  $T$  of 333 K [19], falling or rolling sphere viscometry [11, 14, 36–44], capillary viscometry [50–52, 54], and most studies using concentric cylinder viscometry [10, 12, 45–49, 56]. A few notable outliers could be identified, which holds particularly true for the data reported in the study of Trenzado *et al.* [58]. Their data for  $\eta_L$  obtained by capillary viscometry deviate significantly from all the remaining database with relative deviations of more than  $+60\%$  from Eq. 1, which exceed the scales illustrated in Fig. 3. By trend, systematic negative deviations from  $\eta_{L,calc}$  down to  $-15\%$  are evident for the literature values obtained using cone and plate viscometry [13, 35, 55]. Furthermore, the viscosity data from Seki *et al.* [57] obtained using concentric cylinder viscometry scatter around the SLS-based correlation, with relative deviations between  $-7\%$  and  $+19\%$ . Based on a review of all references, it has been found that the water content of the investigated IL samples has been sufficiently low, thereby excluding the influence of water as a common reason for too low viscosity values of ILs [59]. Overall, the current investigation of the viscosity of [EMIM][NTf<sub>2</sub>] by SLS agrees well with the existing literature and could significantly extend the database towards higher temperatures up to 473 K.

### 4.3 Surface Tension

The experimental data for the surface tension of [EMIM][NTf<sub>2</sub>], obtained from the PD method and denoted by  $\sigma_{PD}$  in Table 1, are represented in Fig. 4 in dependence on temperature. From (303 to 473) K, the measurement results show the typically found, relatively linear decrease with increasing  $T$ . Thus, a linear correlation function with respect to temperature given by

$$\sigma_{calc} = \sigma_0 + \sigma_1 T \quad (2)$$

could be applied. The parameters in Eq. 2 determined from an unweighted fitting procedure are  $\sigma_0 = 50.42 \text{ mN}\cdot\text{m}^{-1}$  and  $\sigma_1 = -0.04772 \text{ mN}\cdot\text{m}^{-1}\cdot\text{K}^{-1}$ . This results in an AARD of the PD data from  $\sigma_{calc}$  of 0.13%. In all cases, the relative deviations of the PD values from  $\sigma_{calc}$  are clearly lower than their uncertainties displayed by the red error bars.

Figure 4 includes also the experimental surface tensions of [EMIM][NTf<sub>2</sub>] obtained from the present SLS experiments (denoted by  $\sigma_{SLS}$  in Table 1) between (353 and 473) K simultaneously with the determined viscosities as well as all previously published data in literature accessed by the IL database “ILThermo” [9].

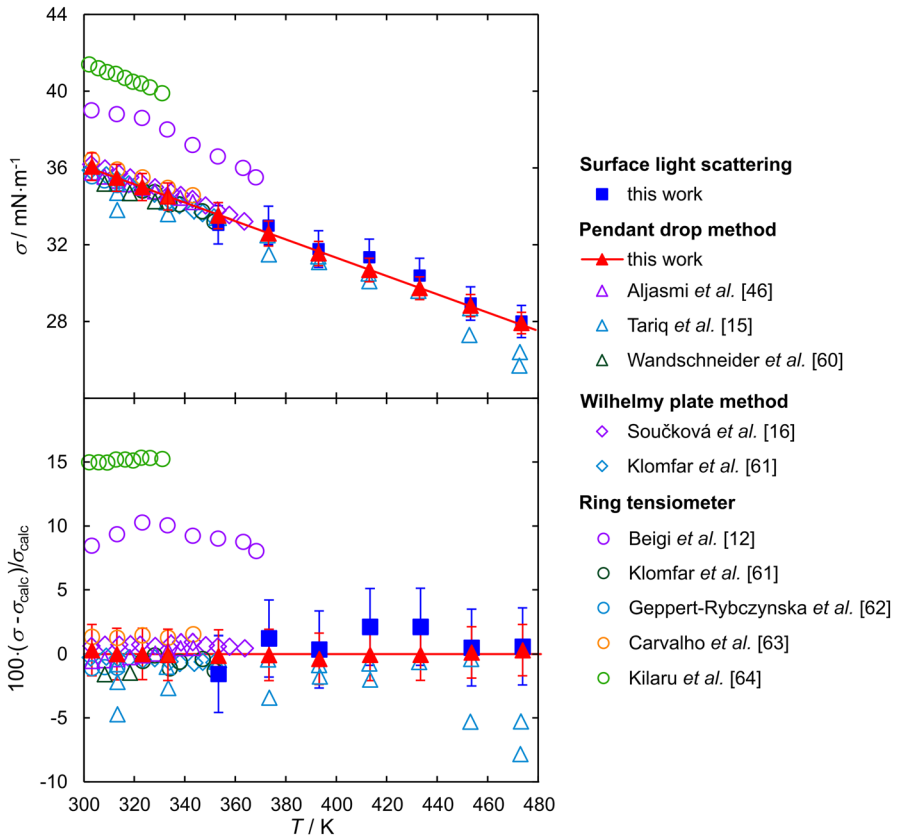


**Fig. 4** Data comparison for surface tension  $\sigma$  of [EMIM][NTf<sub>2</sub>] at 0.1 MPa as a function of temperature  $T$ . The upper part presents the absolute values obtained from the present PD ( $\blacktriangle$ ) and SLS ( $\blacksquare$ ) measurements as well as collected from literature and categorized according to the used measurement technique, while the lower part shows the relative deviations of experimental data from the fit  $\sigma_{\text{calc}}$  (—, Eq. 2) developed from the PD results. Error bars representing the experimental expanded ( $k=2$ ) uncertainties are only shown for the present PD and SLS data (Color figure online)

These ten different datasets featuring at least three single  $T$ -dependent data points are cataloged based on the applied measurement method, which is assigned to a specified marker symbol in Fig. 4. Here, it can be seen that the SLS results show excellent agreement with the results from the PD method within 2 % over the entire temperature range. This demonstrates the reliable access to the surface tension by the SLS technique, even close to the critical damping of surface fluctuations at  $Y$  numbers around 1, where the experiments and the data evaluation are more challenging. The agreement of the  $\sigma$  results also implies that the IL phase boundaries studied by the macroscopic PD method and the microscopic SLS technique are practically identical.

The majority of the literature sources is restricted to the lower temperature range below 373 K. In this range, the datasets related to the PD method [46, 60] and

Wilhelmy plate method [16, 61] as well as most of the surface tension determined by ring tensiometers [61–63] match the present PD data  $\sigma_{\text{calc}}$  mostly within  $\pm 2\%$ , see Fig. 4. Exceptions are the distinctly larger values obtained by Beigi *et al.* [12] and Kilaru *et al.* [64] with the help of ring tensiometers. Since water can practically be excluded as a possible error source for  $\sigma$  of IL [59], it seems that the used measurement devices were not applied properly. For temperatures above 373 K, only Tariq *et al.* [15] employed the PD method for investigations up to 533 K. In the temperature range from (303 to 473) K relevant in this study, the data from Tariq *et al.* [15] are smaller than the present PD results and show some scattering, although the deviations are mostly within combined uncertainties. In summary, the current PD and SLS experiments could also improve the data situation for the surface tension of the IL [EMIM][NTf<sub>2</sub>] in the high-temperature region.

## 5 Conclusions

The present study reported first-time experimental data for the viscosity and surface tension of the common IL [EMIM][NTf<sub>2</sub>] up to elevated temperatures of 473 K. Conventional tensiometry in the form of the PD method was combined with the SLS technique for studying the argon-IL interface within the same measurement cell under identical conditions in the presence of an argon atmosphere at 0.1 MPa from (303 to 473) K. For the entire temperature range, the surface tension could be obtained by the PD method with an expanded ( $k=2$ ) uncertainty of 2%. By SLS, the viscosity could be accessed between (303 and 323) K with an uncertainty of 2.3% using the PD results as an input, while a simultaneous determination of viscosity and surface tension with average uncertainties of 4% and 3% was possible from (353 to 473) K. The sound thermal stability of the IL sample could be confirmed by the matching of the results for both properties from several repetition measurements at 323 K after experiments at high temperatures up to 473 K. The agreement of the surface tension from the PD method and SLS validates the accurate access to this property by both techniques, even close to the critical damping of the surface fluctuations probed by SLS. The relative deviations of the present experimental results and the majority of the available data in literature are typically within 5% and 2% for viscosity and surface tension, respectively. Since the so far existing database is often only available up to about 353 K, the present work serves to extend the thermophysical property database for viscosity and surface tension of ILs at process-relevant elevated temperatures.

**Acknowledgements** The authors gratefully acknowledge funding of the Erlangen Graduate School in Advanced Optical Technologies (SAOT) by the Bavarian State Ministry for Science and Art.

**Author Contributions** ZZ performed the measurements and their evaluation, and wrote the main manuscript text. TMK supervised and coordinated the investigations and wrote the main manuscript text. Both authors reviewed the manuscript.

**Funding** Open Access funding enabled and organized by Projekt DEAL. This work was funded by the Deutsche Forschungsgemeinschaft (DFG, German Research Foundation)–Project-ID 431791331–SFB 1452 (CLINT Catalysis at Liquid Interfaces).

**Data Availability** Not applicable.

## Declarations

**Competing Interests** The authors have no competing interests as defined by Springer, or other interests that might be perceived to influence the results and/or discussion reported in this paper.

**Open Access** This article is licensed under a Creative Commons Attribution 4.0 International License, which permits use, sharing, adaptation, distribution and reproduction in any medium or format, as long as you give appropriate credit to the original author(s) and the source, provide a link to the Creative Commons licence, and indicate if changes were made. The images or other third party material in this article are included in the article's Creative Commons licence, unless indicated otherwise in a credit line to the material. If material is not included in the article's Creative Commons licence and your intended use is not permitted by statutory regulation or exceeds the permitted use, you will need to obtain permission directly from the copyright holder. To view a copy of this licence, visit <http://creativecommons.org/licenses/by/4.0/>.

## References

1. M. Śmiglak, A. Metlen, R.D. Rogers, *Acc. Chem. Res.* **40**, 1182 (2007)
2. P. Wasserscheid, T. Welton (eds.), *Ionic Liquids in Synthesis*, 2nd edn. (Wiley-VCH Verlag GmbH & Co. KGaA, Weinheim, 2007)
3. A. Riisager, R. Fehrmann, S. Flicker, R. van Hal, M. Haumann, P. Wasserscheid, *Angew. Chem. Int. Ed.* **44**, 815 (2005)
4. J.M. Marinkovic, A. Riisager, R. Franke, P. Wasserscheid, M. Haumann, *Ind. Eng. Chem. Res.* **58**, 2409 (2019)
5. M. Hatanaka, T. Yasuda, E. Uchiage, M. Nishida, K. Tominaga, A.C.S. Sustain, *Chem. Eng.* **9**, 11674 (2021)
6. S. Walter, M. Haumann, P. Wasserscheid, H. Hahn, R. Franke, *AIChE J.* **61**, 893 (2015)
7. D. Giovannelli, M.C. Buzzeo, N.S. Lawrence, C. Hardacre, K.R. Seddon, R.G. Compton, *Talanta* **62**, 904 (2004)
8. Y. Cao, T. Mu, *Ind. Eng. Chem. Res.* **53**, 8651 (2014)
9. A. Kazakov, J.W. Magee, R.D. Chirico, E. Paulechka, V. Diky, C.D. Muzny, K. Kroenlein, M. Frenkel, NIST Standard Reference Database 147: NIST Ionic Liquids Database - (ILThermo), version 2.0, National Institute of Standards and Technology, Gaithersburg MD, United States, 20899, <http://ilthermo.boulder.nist.gov>.
10. T. Makino, M. Kanakubo, Y. Masuda, T. Umecky, A. Suzuki, *Fluid Phase Equilib.* **362**, 300 (2014)
11. A. Yadav, A. Guha, A. Pandey, M. Pal, S. Trivedi, S. Pandey, *J. Chem. Thermodyn.* **116**, 67 (2018)
12. A.A.M. Beigi, M. Abdouss, M. Yousefi, S.M. Pourmortazavi, A. Vahid, *J. Mol. Liq.* **177**, 361 (2013)
13. A. Hofmann, M. Migeot, T. Hanemann, *J. Chem. Eng. Data.* **61**, 114 (2016)
14. G. Annat, M. Forsyth, D.R. MacFarlane, *J. Phys. Chem. B* **116**, 8251 (2012)
15. M. Tariq, A.P. Serro, J.L. Mata, B. Saramago, J.M. Esperança, J.N. Canongia Lopes, L.P.N. Rebelo, *Fluid Phase Equilib.* **294**, 131 (2010)
16. M. Součková, J. Klomfar, J. Pátek, *Fluid Phase Equilib.* **333**, 38 (2012)
17. T. Koller, M.H. Rausch, P.S. Schulz, M. Berger, P. Wasserscheid, I.G. Economou, A. Leipertz, A.P. Fröba, *J. Chem. Eng. Data.* **57**, 828 (2012)
18. B. Hasse, J. Lehmann, D. Assenbaum, P. Wasserscheid, A. Leipertz, A.P. Fröba, *J. Chem. Eng. Data.* **54**, 2576 (2009)
19. A.P. Fröba, H. Kremer, A. Leipertz, *J. Phys. Chem. B* **112**, 12420 (2008)

20. A.P. Fröba, S. Will, Light scattering by surface waves - surface light scattering, in *Experimental Thermodynamics, Vol. IX: Advances in Transport Properties of Fluids*, ed. by M.J. Assael, A.H. Goodwin, V. Vesovic, W.A. Wakeham (The Royal Society of Chemistry, Cambridge, 2014), pp. 22–35
21. D. Langevin, *Light Scattering by Liquid Surfaces and Complementary Techniques* (Dekker, Marcel, New York, 1992)
22. Z. Zhai, J.H. Jander, A. Bergen, J. Cui, K. Meyer, T.M. Koller, Int. J. Thermophys. **43**, 178 (2022)
23. Z. Zhai, T.M. Koller, J. Mol. Liq. **377**, 121491 (2023)
24. Z. Zhai, U. Paap, A. Gezmis, F. Maier, H.-P. Steinrück, T.M. Koller, J. Mol. Liq. (2023). <https://doi.org/10.1016/j.molliq.2023.122388>
25. A.P. Fröba, *Simultane Bestimmung von Viskosität und Oberflächenspannung transparenter Fluide mittels Oberflächenlichtstreuung*, Dr.-Ing. Thesis, Friedrich-Alexander-Universität Erlangen-Nürnberg, 2002
26. A.I. Rusanov, V. Prokhorov, *Interfacial Tensiometry* (Elsevier, Amsterdam, 1996)
27. E.H. Lucassen-Reynders, J. Lucassen, Adv. Colloid Interface Sci. **2**, 347 (1970)
28. S.M. Saad, A.W. Neumann, Adv. Colloid Interface Sci. **238**, 62 (2016)
29. M. Kerscher, J.H. Jander, J. Cui, M.M. Martin, M. Wolf, P. Preuster, M.H. Rausch, P. Wasserscheid, T.M. Koller, A.P. Fröba, Int. J. Hydrog. Energy **47**, 15789 (2022)
30. T.M. Koller, M. Kerscher, A.P. Fröba, J. Colloid Interf. Sci. **626**, 899 (2022)
31. E.W. Lemmon, I.H. Bell, M.L. Huber, M.O. McLinden, *NIST Standard Reference Database 23: Reference Fluid Thermodynamic and Transport Properties (REFPROP)*, version 10.0; National Institute of Standards and Technology, 2018
32. V. Seidl, M. Bosch, U. Paap, M. Livraghi, Z. Zhai, C.R. Wick, T.M. Koller, P. Wasserscheid, F. Maier, A.-S. Smith, J. Bachmann, H.-P. Steinrück, K. Meyer, J. Ionic Liq. **2**, 100041 (2022)
33. S.-H. Liu, C.-C. Chen, B. Zhang, J.-H. Wu, RSC Adv. **10**, 22468 (2020)
34. H.L. Ngo, K. LeCompte, L. Hargens, A.B. McEwen, Thermochim. Acta **357–358**, 97 (2000)
35. J.J. Fillion, J.F. Brennecke, J. Chem. Eng. Data **62**, 1884 (2017)
36. K.R. Harris, M. Kanakubo, J. Chem. Eng. Data **66**, 4618 (2021)
37. S. Doblinger, D.S. Silvester, M. CostaGomes, Fluid Phase Equilib. **549**, 113211 (2021)
38. E.P. Yambou, B. Gorska, F. Béguin, J. Mol. Liq. **298**, 111959 (2020)
39. R. Khalil, N. Chaabene, M. Azar, I.B. Malham, M. Turmine, Fluid Phase Equilib. **503**, 112316 (2020)
40. N. Chaabene, K. Ngo, M. Turmine, V. Vivier, J. Mol. Liq. **319**, 114198 (2020)
41. Q. Liu, L. Zhao, Q. Zheng, L. Mou, P. Zhang, J. Chem. Eng. Data. **63**, 4484 (2018)
42. A. Kadyan, S. Pandey, J. Chem. Thermodyn. **116**, 159 (2018)
43. N. Anwar, Riyazuddeen, S. Yasmeen, J. Mol. Liq. **224**, 189 (2016)
44. R. Salinas, J. Pla-Franco, E. Lladosa, J.B. Montón, J. Chem. Eng. Data. **60**, 525 (2015)
45. M. Tariq, P.J. Carvalho, J.A. Coutinho, I.M. Marrucho, J.N.C. Lopes, L.P.N. Rebelo, Fluid Phase Equilib. **301**, 22 (2011)
46. A. Aljasmí, A.S. AlJimaz, K.H. AlKhaldi, M.S. AlTuwaím, J. Chem. Eng. Data **67**, 858 (2022)
47. Q. Liu, L. Ma, S. Wang, Z. Ni, X. Fu, J. Wang, Q. Zheng, J. Mol. Liq. **325**, 114573 (2021)
48. M.L. Batista, L.I. Tomé, C.M. Neves, J.R. Gomes, J.A. Coutinho, J. Mol. Liq. **192**, 26 (2014)
49. J.M. Vuksanovic, M.S. Calado, G.R. Ivanis, M.L. Kijevcanin, S.P. Serbanovic, Z.P. Visak, Fluid Phase Equilib. **352**, 100 (2013)
50. S. Papović, M. Bešter-Rogač, M. Vraneš, S. Gadžurić, J. Chem. Thermodyn. **99**, 1 (2016)
51. R.G. Seoane, S. Corderí, E. Gómez, N. Calvar, E.J. González, E.A. Macedo, Á. Domínguez, Ind. Eng. Chem. Res. **51**, 2492 (2012)
52. C. Schreiner, S. Zugmann, R. Hartl, H.J. Gores, J. Chem. Eng. Data. **55**, 1784 (2010)
53. A. Ahosseini, A.M. Scurto, Int. J. Thermophys. **29**, 1222 (2008)
54. H. Yao, S. Zhang, J. Wang, Q. Zhou, H. Dong, X. Zhang, J. Chem. Eng. Data **57**, 875 (2012)
55. D.W. Bruce, C.P. Cabry, J.N.C. Lopes, M.L. Costen, L. D'Andrea, I. Grillo, B.C. Marshall, K.G. McKendrick, T.K. Minton, S.M. Purcell, S. Rogers, J.M. Slattery, K. Shimizu, E. Smoll, M.A. Tesar-Serrate, J. Phys. Chem. B **121**, 6002 (2017)
56. L.M. Ramenskaya, E.P. Grishina, N.O. Kudryakova, J. Mol. Liq. **272**, 759 (2018)
57. S. Seki, T. Kobayashi, Y. Kobayashi, K. Takei, H. Miyashiro, K. Hayamizu, S. Tsuzuki, T. Mitsugi, Y. Umebayashi, J. Mol. Liq. **152**, 9 (2010)
58. J.L. Trenzado, Y. Rodríguez, A. Gutiérrez, A. Cincotti, S. Aparicio, J. Mol. Liq. **334**, 116049 (2021)

59. A.P. Fröba, P. Wasserscheid, D. Gerhard, H. Kremer, A. Leipertz, *J. Phys. Chem. B* **111**, 12817 (2007)
60. A. Wandschneider, J.K. Lehmann, A. Heintz, *J. Chem. Eng. Data* **53**, 596 (2008)
61. J. Klomfar, M. Součková, J. Pátek, *J. Chem. Thermodyn.* **42**, 323 (2010)
62. M. Geppert-Rybczyńska, J.K. Lehmann, A. Heintz, *J. Chem. Eng. Data* **56**, 1443 (2011)
63. P.J. Carvalho, M.G. Freire, I.M. Marrucho, A.J. Queimada, J.A.P. Coutinho, *J. Chem. Eng. Data* **53**, 1346 (2008)
64. P. Kilaru, G.A. Baker, P. Scovazzo, *J. Chem. Eng. Data* **52**, 2306 (2007)

**Publisher's Note** Springer Nature remains neutral with regard to jurisdictional claims in published maps and institutional affiliations.

## Authors and Affiliations

Ziwen Zhai<sup>1</sup> · Thomas M. Koller<sup>1</sup> 

✉ Thomas M. Koller  
thomas.m.koller@fau.de

<sup>1</sup> Institute of Advanced Optical Technologies - Thermophysical Properties (AOT-TP), Department of Chemical and Biological Engineering (CBI) and Erlangen Graduate School in Advanced Optical Technologies (SAOT), Friedrich-Alexander-Universität Erlangen-Nürnberg (FAU), Paul-Gordan-Straße 8, 91052 Erlangen, Germany